European Rotorcraft Forum

BOUNDARY INTEGRAL FORMULATIONS FOR NOISE SCATTERED BY HELICOPTER FUSELAGE

Caterina Poggi, caterina.poggi@uniroma3.it, University Roma Tre (Italy)
Giovanni Bernardini, g.bernardini@uniroma3.it, University Roma Tre (Italy)
Claudio Testa, claudio.testa@cnr.it, CNR-INM (Italy)
Massimo Gennaretti, m.gennaretti@uniroma3.it, University Roma Tre (Italy)

Abstract
The paper deals with a theoretical-numerical comparison among integral formulations for the prediction of noise scattered by moving bodies. Three acoustic scattering integral formulations for the solution of the velocity potential wave equation are considered: a recently proposed linearized boundary-field integral formulation, and two widely applied boundary integral approaches based on Taylor and Taylor-Lorentz transformations. Aim of the work is to highlight their theoretical differences and limits of applicability, while examining their capability of capturing the influence of body motion and corresponding nonuniform mean flow around it on the scattered noise field. Numerical results concern a rigid translating sphere impinged by sound waves emitted by a co-moving pulsating point-source and a helicopter fuselage impinged by noise radiated by main- and tail-rotor.

1. INTRODUCTION

Sound scattering occurs when an obstacle (scatterer) is present in the path of an acoustic wave and produces secondary sound spread in a variety of directions. Under the assumption that the wavelength of the impinging sound is comparable or less than a characteristic size of the scatterer, the acousto-structural interaction causes a redistribution of the energy content of the impinging wave into reflected and diffracted secondary waves that may remarkably alter magnitude, waveform and directivity of the overall noise field with respect to the unbounded space propagation. This phenomenon is relevant for a wide range of engineering applications dealing with stationary and moving objects: for instance, in aeronautics, to determine the sources of airborne and structure-borne cabin noise, as well as, to predict far field noise distribution affecting populated areas; in hydroacoustic ship design, to limit the impact of sea acoustic pollution on marine life, to comply with noise emission regulations and limitation of acoustic detectability of warships.

Basically, the analysis of acoustic scattering is conceived as a a two-step problem where the impinging pressure wave emitted by the main source of sound is considered frozen, namely independent of the presence of the scattering surface. The incident sound field (which represents the input for this type of problems) may be thus computed by prior hydro/aerodynamic and hydro/aeroacoustic analyses of the emitting source, as if it were isolated, with the total noise field divided into incident and scattered components: this assumption permits to avoid time-consuming computations for the coupled analysis of primary source and scatterer of sound. For instance, this approach may be successfully applied to capture acoustic scattering effects from fuselage/wing/rudder components of propeller-driven aircraft in cruise flight, where propeller aerodynamics is scarcely affected by the rest of the configuration[1], and to predict the acoustic shielding effects of helicopter cabins in flight conditions characterized by the absence of relevant aerodynamic interactions with the main-rotor wake[2]. Differently, marine configurations with thrusting propellers behind the hull inherently suffer of the hydrodynamic interaction between turbulent and vorticity fields released by the hull. However, for cruising motion without interactions between vortex structures and propeller blades, fully-appended hull scattering effects may be computed by considering isolated propellers working in a non-homogeneous onset-flow given by a prior hydrodynamic analysis of the moving hull[3].

Literature papers show that the scattered pressure field is typycally predicted by the solution of

linear boundary integral formulations that solve the Helmholtz equation for the velocity potential or the acoustic pressure.[4,5,6,7] Alternative approaches propose the application of the Acoustic Analogy in a non-standard fashion that extends the integral solution of the linear version of the Ffowcs Williams and Hawkings Equation (FWHE)[8,9,10,11] to scattering problems. Common feature of these formulations is the application of a Boundary Element Method (BEM) to determine, first, the scattered pressure upon the scatterer surface by solution of a boundary integral equation and, then to evaluate the scattered noise in the flowfield by the corresponding boundary integral representation. By assuming inviscid potential compressible subsonic flows, the Helmholtz formulations, namely, the velocity potential approach (VP) and the Lighthill Equation for the acoustic pressure (LE), along with the linear FWHE formulation, provide fully equivalent results as long as the scattering body is at rest, wheres relevant discrepancies may arise when the body moves.[12,13] Indeed, these linear models consider acoustic propagation in homogeneous medium at rest, thus neglecting the effects of nonuniform flow component arising when the scatterer is in relative motion with respect to the fluid. The consideration of these effects on wave radiation would require the inclusion of the nonlinear field terms that they ignore.

In previous works, a boundary-field formulation including the linearized field source-terms contribution has been developed and the corresponding predictions have been compared with those obtained by the linear formulations for a moving noise scattering wing.[12,13] Specifically, a frequency-domain boundary-field integral formulation has been developed for the velocity potential by extracting from the source field terms the first-order perturbations with respect to the steady velocity potential associated to the uniform translation of the scatterer.[12] Numerical investigations highlighted the significant influence of the field linearized sources to the directivity pattern of the scattered sound. Differently, the scattering problem could be stated in terms of boundary integral formulations for the solution of the Lighthill and Ffowcs Williams and Hawkings Equations on a fictitious permeable surface surrounding the scatterer and co-moving with it and embedding the corresponding noise field sources.[13] This approach allows to avoid cumbersome computations of volume integrals involving the Lighthill stress tensor, that may be impracticable for high-frequency simulations of realistic three-dimensional configurations. Numerical results demonstrate the desired matching among the examined scattering formulations for moving objects (namely, VP, LE and FWH), thus confirming, at the same time, their perfect equivalence when their complete versions are applied, and the different acoustic effects induced by the corresponding field source terms. Last but not least, note that the approaches based on the definition of permeable surfaces are not autonomous, in that require the knowledge of suitable input data on the permeable surface provided by a prior very near field acosutic solution. This is an unavoidable drawback of pressure-based formulations for the scattering analysis of moving bodies in the presence of not negligible mean-flow effects, that marks the difference with respect to the velocity potential boundary-field integral formulation.

Although the aforementioned scattering models provide an accurate description of nonuniform mean flow effects on the sound field generated by scattering bodies, their application is actually not so straightforward due to the required evaluation of the field sources of sound localized around the scatterer. However, if the interest is on weakly nonuniform mean flows with characteristic length-scales comparable with (or larger than) the characteristic length-scales of the acoustic disturbance, the noise scattered by moving bodies may be conveniently captured by applying, linear boundary integral formulations that, for homentropic potential flows, solve suited non-homogeneous forms of the wave equation for the velocity potential in the Taylor or Taylor-Lorentz transformed spaces.[14,15,16] These boundary integral formulations for the noise scattered in the presence of moving bodies and nonuniform mean flow are widely applied and the purpose of the present paper is the theoretical-numerical comparison among them and the linearized boundary-field integral approach in order to identify the common aspects of the different formulations, as well as, their limits of applicability and order of accuracy.

The paper is structured as follows: the equations governing the potential field in the presence of a moving perturbation source are briefly presented, then Section 2.1 outlines the novel boundary-field integral scattering formulation,[12] whereas Sections 2.2 and 2.3 show the basic features of the scattering formulations involving the Taylor and Taylor-Lorentz transforms. Comparisons among the numerical predictions obtained by these three formulations are shown in Section 3.1, concerning the analysis of the noise scattered by a sphere in uniform rectilinear translation impinged by the sound emitted by a pulsating co-moving monopole. Next, the main- and tail-rotor noise scattered by a helicopter fuselage is examined by both Taylor and Taylor-Lorentz boundary integral formulations in Section 3.2. The configuration considered is that

tested in the HART II project[20,21,22], which is a joint multi-national program aimed at performing extensive wind tunnel measurements concerning aerodynamics and aeroacoustics of a four-bladed model rotor in low-speed descent flight, placed above a realistic fuselage model. The conclusions are discussed in Section 4.

2. SOUND SCATTERING MODELLING FOR MOVING BODIES

For an inviscid, isentropic and irrotational flow at rest, the velocity field $\mathbf{v}$ is given by the gradient of the velocity potential ϕ, that is, $\mathbf{v} = \nabla\phi$. Then, let us consider a body with surface $\mathcal{S}$ that translates at uniform velocity $\mathbf{v}_B$ respect to a frame of reference fixed with the undisturbed medium. If an external source of intensity $A_i(t)$ located at the point $\mathbf{x}_i(t)$ generates a perturbation velocity potential field impinging $\mathcal{S}$, the propagation of the total potential described in a frame of reference rigidly connected with the body (body frame of reference, BFR), is governed by[17]

$$\nabla^2\phi - \frac{1}{c_0^2}\left(\frac{\partial}{\partial t} - \mathbf{v}_B\cdot\nabla\right)^2\phi = \\ = \sigma(\phi) + A_i\,\delta(\mathbf{x}-\mathbf{x}_i) \tag{1}$$

where c_0 denotes the speed of sound in the undisturbed medium, and

$$\sigma(\phi) = \left(1-\frac{c^2}{c_0^2}\right)\nabla^2\phi \\ + \frac{1}{c_0^2}\left(\frac{\partial v^2}{\partial t} - \mathbf{v}_B\cdot\nabla v^2\right) + \frac{\mathbf{v}}{2c_0^2}\cdot\nabla v^2 \tag{2}$$

collects all the nonlinear terms, with c denoting the local speed of sound.

2.1. Boundary-field formulation for the velocity potential (VP)

Following the boundary integral equation method,[17,18] the solution of Eq. 1 is given by the following boundary-field expression

$$\phi(\mathbf{x},t) = \int_{\mathcal{S}}\left[G_0\frac{\partial\phi}{\partial\tilde{n}} - \phi\frac{\partial G_0}{\partial\tilde{n}}\right]\mathrm{d}\mathcal{S}(\mathbf{y}) \\ + \int_{\mathcal{S}}\left[\frac{\partial\phi}{\partial t}\,G_0\left(\frac{\partial\theta}{\partial\tilde{n}} + 2\frac{\mathbf{M}\cdot\mathbf{n}}{c_0}\right)\right]\mathrm{d}\mathcal{S}(\mathbf{y}) \\ + \int_{\mathcal{V}} G_0\,[\sigma]_\theta\,\mathrm{d}\mathcal{V}(\mathbf{y}) + \phi_i(\mathbf{x},t) \tag{3}$$

where $\mathcal{V}$ represents a field domain surrounding the body where the nonlinear terms are not negligible. In this integral equation $G_0(\mathbf{x},\mathbf{y}) = -1/4\,\pi\,r_\beta$, with $r_\beta = \sqrt{[\mathbf{M}\cdot(\mathbf{y}-\mathbf{x})]^2 + \beta^2||\mathbf{y}-\mathbf{x}||^2}$ and $\beta^2 = (1-\mathbf{M}\cdot\mathbf{M})$, with $\mathbf{M} = \mathbf{v}_B/c_0$ denoting the body velocity Mach number. The symbol $[\ldots]_\theta$ means evaluation at retarded time, $t-\theta$, where $\theta = 1/(c_0\beta^2)[r_\beta - \mathbf{M}\cdot(\mathbf{y}-\mathbf{x})]$ represents the acoustic time delay (namely, the time taken by a perturbation emitted in $\mathbf{y}$ to reach $\mathbf{x}$). In addition, $\partial(\cdot)/\partial\hat{n} = \partial(\cdot)/\partial n - \mathbf{M}\cdot\mathbf{n}\,\mathbf{M}\cdot\nabla(\cdot)$ with $\mathbf{n}$ denoting the body outward unit normal vector, whereas $\phi_i(\mathbf{x},t) = [A_i\,G_0(\mathbf{x},\mathbf{x}_i)]_\theta$ represents the value of the velocity potential field generated by the perturbation source.

For ϕ_{st} and ϕ_s denoting, respectively, the steady-state velocity potential field due to the uniform translation of the body and the unsteady potential scattered by the body as a consequence of the incident field ϕ_i, the total potential may be split into $\phi = \phi_{st} + \phi_s + \phi_i$. Thus, assuming $\phi_p = \phi_s + \phi_i$ as a small perturbation with respect to ϕ_{st}, the linearization process about ϕ_{st} yields the following boundary-field integral equation for ϕ_s in the Fourier domain[12]

$$\tilde{\phi}_s(\mathbf{x}) = \int_{\mathcal{S}} G\left(-\frac{\partial\tilde{\phi}_i}{\partial n} - \mathbf{M}\cdot\mathbf{n}\,\mathbf{M}\cdot\nabla\tilde{\phi}_s\right)\mathrm{d}\mathcal{S}(\mathbf{y}) \\ + \int_{\mathcal{S}}\left(-\tilde{\phi}_s\frac{\partial G}{\partial\tilde{n}} + 2\,\mathbf{M}\cdot\mathbf{n}\,jk\,\tilde{\phi}_s\,G\right)\mathrm{d}\mathcal{S}(\mathbf{y}) \\ + \int_{\mathcal{V}} G\,\tilde{\mu}\,\mathrm{d}\mathcal{V}(\mathbf{y}) \tag{4}$$

derived through imposition of the steady and unsteady flow impermeability boundary conditions, namely $\partial\phi_0/\partial n = \mathbf{v}_B\cdot\mathbf{n}$ and $\partial\phi_s/\partial n = -\partial\phi_i/\partial n$. In Eq. 4 $\tilde{(\cdot)}$ means Fourier transformation, $k = \omega/c_0$ is the wave number of the impinging field, whilst G is given by

$$G(\mathbf{x},\mathbf{y}) = \frac{-1}{4\,\pi\,r_\beta}\exp\left[-jk\left(\frac{r_\beta + M_\infty\Delta x}{\beta^2}\right)\right] \tag{5}$$

where, for $\mathbf{M} = -M_\infty\mathbf{i}$, $M_\infty\Delta x = -\mathbf{M}\cdot(\mathbf{y}-\mathbf{x})$. Here, the time-delay is related to wave propagation through uniform flow, whereas the effects of nonuniform mean flow are taken into account by the volume field term, $\tilde{\mu}$, derived as the first-order approximation of the perturbation of the nonlinear terms, σ, about their steady-state value, σ_0[12]. Specifically

$$\tilde{\mu} = A_1\nabla^2\tilde{\phi}_p + jk\,A_2\,\tilde{\phi}_p + (\mathbf{A}_3 + jk\,\mathbf{A}_4)\cdot\nabla\tilde{\phi}_p \\ + \mathbf{A}_5\cdot\nabla\left(\mathbf{v}_{st}\cdot\nabla\tilde{\phi}_p\right) \tag{6}$$

with $A_1, A_2, \mathbf{A}_3, \mathbf{A}_4, \mathbf{A}_5$ denoting constant coefficients that depend on the nonuniform mean flow

velocity, $\mathbf{v}_{st} = \nabla\phi_{st}$,

$$
\begin{aligned}
A_1 &= \frac{\gamma-1}{{c_0}^2}\left(\frac{v_{st}^2}{2} - \mathbf{v}_B \cdot \mathbf{v}_{st}\right)\\
A_2 &= \frac{\gamma-1}{{c_0}^2}\nabla^2\phi_{st}\\
\mathbf{A}_3 &= \frac{1}{{c_0}^2}\left[\frac{\nabla {v_{st}}^2}{2} + (\gamma+1)(\mathbf{v}_{st}-\mathbf{v}_B)\nabla^2\phi_{st}\right]\\
\mathbf{A}_4 &= \frac{2}{{c_0}^2}\mathbf{v}_{st}\\
\mathbf{A}_5 &= \frac{1}{{c_0}^2}(\mathbf{v}_{st} - 2\,\mathbf{v}_B)
\end{aligned}
\tag{7}
$$

with γ denoting the ratio of specific heat coefficients c_p/c_v.

2.2. Boundary formulation based on Taylor-Lorentz transformation (TL)

For L_A and L_M representing the characteristic length scales of acoustic and mean flow fields, respectively, performing an ordering scheme of the nonlinear terms in Eq. 1 for which only terms of the order $[\phi]/L_A^2$, $M_\infty[\phi]/L_A^2$, $M_\infty^2[\phi]/L_A^2$, $M_\infty^2[\phi]/L_A L_M$ are retained with $L_A \leq L_M$ and $M_\infty << 1$, and assuming a weakly non-uniform mean flow, namely a flow where the non-uniform component $\mathbf{v}_{st}/c_0$ is small compared to M_∞, the equation governing the potential field in the presence of a moving body and a source of perturbations reads[15,16]

$$
\begin{aligned}
&\nabla^2\phi - \frac{1}{c_0^2}\left(\frac{\partial}{\partial t} - \mathbf{v}_B\cdot\nabla\right)^2\phi\\
&-\frac{2}{c_0^2}\mathbf{v}_{st}\cdot\frac{\partial\nabla\phi}{\partial t} = A_i\,\delta(\mathbf{x}-\mathbf{x}_i)
\end{aligned}
\tag{8}
$$

Next, the application of the Taylor-Lorentz transformation recasts Eq. 8 into the standard wave equation[16] which, in the frequency domain, is solved by the following boundary integral equation

$$
\begin{aligned}
\tilde{\phi}_s(\mathbf{x}) &= \int_{\mathcal{S}} G_{TL}\left(-\frac{\partial\tilde{\phi}_i}{\partial n}\right)\mathrm{d}\mathcal{S}(\mathbf{y})\\
&- \int_{\mathcal{S}} G_{TL}\mathbf{M}\cdot\mathbf{n}\mathbf{M}\cdot\nabla\tilde{\phi}_s\mathrm{d}\mathcal{S}(\mathbf{y})\\
&- \int_{\mathcal{S}}\tilde{\phi}_s\left(\frac{\partial G_{TL}}{\partial\tilde{n}} + 2\mathbf{M}_0\cdot\mathbf{n}jkG_{TL}\right)\mathrm{d}\mathcal{S}(\mathbf{y})
\end{aligned}
\tag{9}
$$

where $\mathbf{M}_0 = -\mathbf{M} + \mathbf{v}_{st}/c_0$ is the local Mach number and G_{TL} denotes the approximate fundamental solution of Eq. 8 in the physical space given by

$$
\begin{aligned}
G_{TL}(\mathbf{x},\mathbf{y}) = \frac{-1}{4\,\pi\,r_\beta}\exp\Bigg[-jk\Bigg(&\frac{r_\beta + M\Delta x}{\beta^2}\\
&+\frac{\phi_{st}(\mathbf{y})-\phi_{st}(\mathbf{x})}{c_0}\Bigg)\Bigg]
\end{aligned}
\tag{10}
$$

Differently from Section 2.1, no field acoustic sources are present (thus avoiding the evaluation of volume integral contributions), and weakly nonuniform mean flow effects on the scattered acoustic signal are taken into account only by surface integral contributions.

2.3. Boundary formulation based on Taylor transformation (T)

An alternative acoustic scattering approach valid for low-Mach number analyses comes from the elimination of terms of order M_∞^2 in Eq. 8, which yields[14]

$$
\begin{aligned}
&\nabla^2\phi - \frac{1}{c_0^2}\frac{\partial^2\phi}{\partial t^2} - \frac{2}{c_0^2}(\mathbf{v}_{st}-\mathbf{v}_B)\cdot\frac{\partial\nabla\phi}{\partial t}\\
&= A_i\,\delta(\mathbf{x}-\mathbf{x}_i)
\end{aligned}
\tag{11}
$$

Then, the application of the Taylor transform to Eq. 11, followed by application of the boundary integral equation approach provides, in the physical space[14,15]

$$
\begin{aligned}
\tilde{\phi}_s(\mathbf{x}) = &\int_{\mathcal{S}}\left[-G_T\frac{\partial\tilde{\phi}_i}{\partial n} - \tilde{\phi}_s\frac{\partial G_T}{\partial n}\right]\mathrm{d}\mathcal{S}(\mathbf{y})\\
&+\int_{\mathcal{S}}\left[-2\,\mathbf{M}_0\cdot\mathbf{n}\,jk\,\tilde{\phi}_s\,G_T\right]\mathrm{d}\mathcal{S}(\mathbf{y})
\end{aligned}
\tag{12}
$$

where the approximate fundamental solution of Eq. 11 is expressed as

$$
\begin{aligned}
G_T(\mathbf{x},\mathbf{y}) = \frac{-1}{4\,\pi\,r}\exp\Bigg[-jk\Bigg(&r + M\Delta x\\
&+\frac{\phi_{st}(\mathbf{y})-\phi_{st}(\mathbf{x})}{c_0}\Bigg)\Bigg]
\end{aligned}
\tag{13}
$$

with r denoting the distance between $\mathbf{x}$ and $\mathbf{y}$.

2.4. Theoretical Remarks

The above formulations provide different levels of simulation accuracy for the analysis of sound scattering problems dealing with by moving bodies. As a function of scatterer velocity and of mean flow nonuniformity, the acoustic radiation is predicted by VP, TL and T formulations with reduced levels of accuracy, moving from VP to T ones.

The main differences among the mentioned approaches for sound scattering analysis are:

- the VP formulation requires the evaluation of acoustic field terms in a suitable volume surrounding the body, differently from the TL and T models which require only the evaluation of surface integrals;
- time-delays involved in the VP formulation are related to sound waves traveling in uniform flows. Nonuniform mean flow acoustic effects are taken into account through field sources volume terms;
- time-delays in the TL and T formulations are affected by the nonuniform mean flow effects;
- the validity of the VP formulation is not limited to small Mach number and weakly nonuniform mean flows, whereas the TL model is valid for moderate Mach number and weakly nonuniform flows, and the T formulation is applicable under the assumption of low Mach number and weakly nonuniform flows.

Following the mathematical processes leading to Eqs. 1, 8 and 11 and their integral solutions, one observes that the Green function used in Eq. 5 corresponds to the exact fundamental solution of the adjoint operator associated to the wave equation in uniform mean flow (namely, the homogeneous form of Eq. 1). Differently, Eqs. 10 and 13 represent approximate fundamental solutions of their respectively differential operators. This implies also that the incident potential field produced by the moving pulsating source is not perfectly compatible with the boundary integral representations in Eqs. 9 and 12.

Observing the advantages and disadvantages of the formulations examined suggests the introduction of a further formulation derived by neglecting all the nonlinear terms in Eq. 2 except $(\partial v^2/\partial t)/c_0^2$, thus transforming Eq. 1 into Eq. 8. Then, the application of the integral approach in Section 2.1 with the Green function given by the exact fundamental solution in Eq. 5 yields an integral equation where only the volume contribution of $\mathbf{A}_4$ of Eqs. 7 is retained. Next, neglecting the term related to $\nabla \cdot \mathbf{M}_{st}$ (to comply with the approximation of the TL formulation) and applying the Gauss theorem, the following boundary-field solution in the frequency domain is obtained

$$
\begin{aligned}
\tilde{\phi}_s(\mathbf{x}) = & \int_{\mathcal{S}} G \left(-\frac{\partial \tilde{\phi}_i}{\partial n} - \mathbf{M}\cdot\mathbf{n}\,\mathbf{M}\cdot\nabla\tilde{\phi}_s \right) \mathrm{d}\mathcal{S}(\mathbf{y}) \\
& - \int_{\mathcal{S}} \left[\tilde{\phi}_s \frac{\partial G}{\partial \tilde{n}} + 2\,\mathbf{M}_0\cdot\mathbf{n}\, jk\, \tilde{\phi}_s\, G \right] \mathrm{d}\mathcal{S}(\mathbf{y}) \\
& - \int_{\mathcal{S}} 2\,\mathbf{M}_{st}\cdot\mathbf{n}\, jk\, \tilde{\phi}_i\, G\, \mathrm{d}\mathcal{S}(\mathbf{y}) \\
& - \int_{\mathcal{V}} 2\, jk\, \left(\tilde{\phi}_i + \tilde{\phi}_s\right) \nabla G \cdot \mathbf{M}_{st}\, \mathrm{d}\mathcal{V}(\mathbf{y})
\end{aligned}
\tag{14}
$$

In principle, this approach would lead to a formulation exactly equivalent with the TL one, but the use of Eq. 5 (namely, an exact fundamental solution) determines the presence of a volume contribution that is not present in Eq. 9. Correspondingly, Eqs.9 and 14 have different levels of accuracy. In the following the boundary-field solution given by Eq. 14 is referred to as VP-A4 formulation.

3. NUMERICAL RESULTS

In this section, a numerical investigation on the scattering of a translating sphere impinged by a co-moving pulsating source is presented, as well as a numerical analysis pertaining the fuselage scattering effects on the noise radiated by the main and the tail rotor of the BO-105 scaled model investigated within the HART II program.

3.1. Sound scattered by a rigid sphere

The scattering problem selected to compare the above formulations consists of a sphere with radius $a = 1$ in uniform rectilinear translation, impinged by an incident pressure field due to a co-moving ω-harmonic potential point source. Introducing a

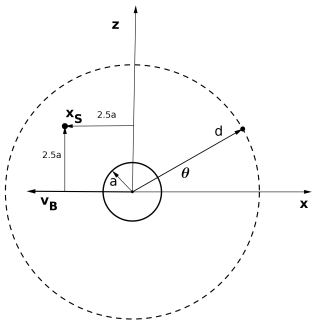

Figure 1: Mid-plane of the scattering sphere. Sphere velocity and location of point source and observers.

coordinate system $(\mathbf{x}_0, x, y, z)$ with origin coinciding with the center of the sphere and fixed with it (see figure 1), let the source position be identified by $\mathbf{x}_S = (-2.5a, 0, 2.5a)$. Moreover, let assume that the sphere moves towards the negative x-axis direction. Acoustic scattering predictions are presented in terms of Sound Pressure Level (SPL) and directivity pattern of the acoustic pressure $p' = p_s + p_i$, evaluated at microphones located at a radial distance $d/a = 3$ from $\mathbf{x}_0$, lying on the plane $y = 0$. First, the assessment of the sensitivity on both Mach number and wave number of the predictions provided by the linear VP, TL, T and linearized VP formulations is presented. To this aim, Figs. 2, 3 show the comparison among them in terms of SPL for M_∞ ranging from 0.1 to 0.4, at two wave numbers $\omega/c_0 = 2$ and $\omega/c_0 = 5$. Volume extensions and surface/volume meshes used for this analysis are such to assure converged results; a dedicated analysis, not shown here for conciseness, highlights that a computational grid of 10000 panels on the body surface and 120000 cells around the sphere used to discretize an external volume extending up to a distance of one radius from the sphere surface guarantees acoustic results insensitive to further mesh refinements (for all the formulations investigated). The aeroacoustic computations are based upon an aerodynamic steady-state solution obtained through a compressible potential-flow boundary integral formulation, suited for the aerodynamic analysis of lifting and non-lifting bodies in unsteady arbitrary motion[17]. As expected, the higher the Mach number and frequency of the impinging noise, the more relevant are the discrepancies between the signals predicted by the boundary integral formulations (namely, T, TL and linear VP) and those provided by the boundary-field linearized VP approach. In other words, the agreement among the acoustic results based on the T, TL, linear VP and boundary-field linearized VP models is good as long as the Mach number of the translating sphere and the frequency of the emitting monopole are low enough; their increase worsens the agreement because of the increased nonuniform mean flow effects. From these results it seems to be mandatory the inclusion of M_∞^2-order terms to maintain accuracy also at very low Mach numbers: indeed the T formulation provides inaccurate results starting from $M_\infty = 0.2$, whereas the inclusion of such contributions gives rise to limited differences with respect to the VP linearized formulation up to about $M_\infty = 0.3$, especially for $\omega/c_0 = 2$. Similar considerations may be done looking at Fig. 4 which shows the comparison between the aforementioned four formulations in terms of directivity pattern of acoustic pressure, at $M_\infty = 0.4$

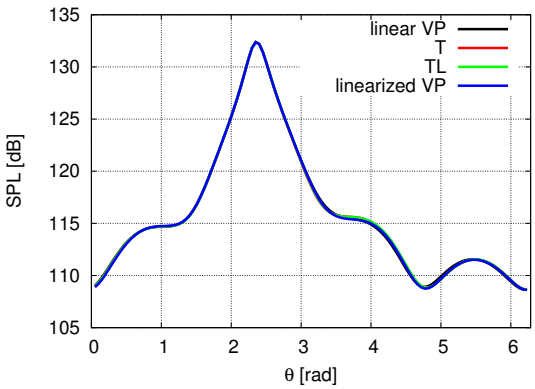

(a) $M = 0.1$

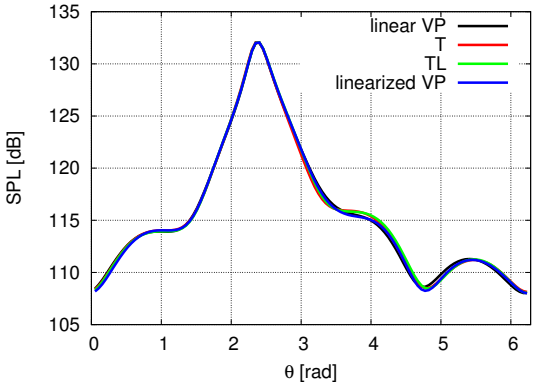

(b) $M = 0.2$

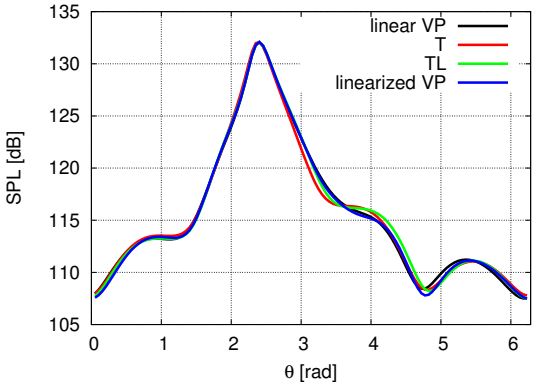

(c) $M = 0.3$

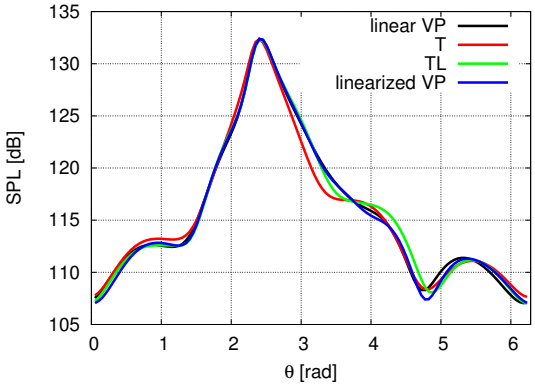

(d) $M = 0.4$

Figure 2: SPL of the acoustic pressure for $\omega/c_0 = 2$.

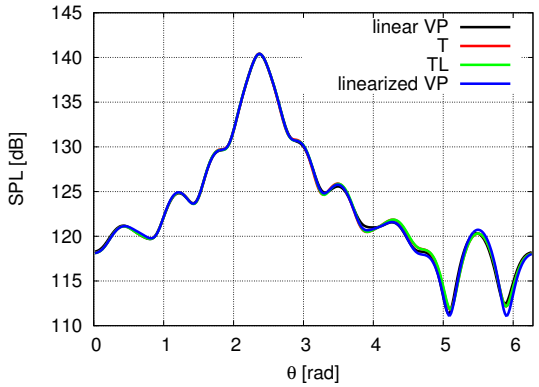

(a) $M = 0.1$

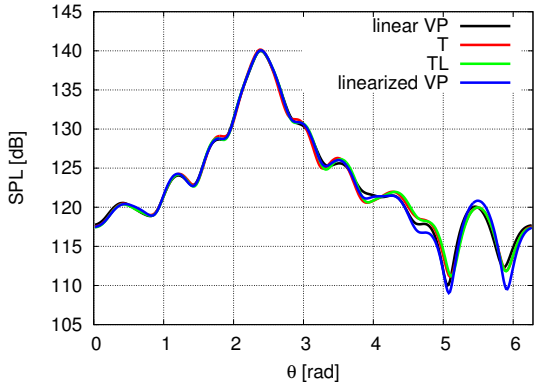

(b) $M = 0.2$

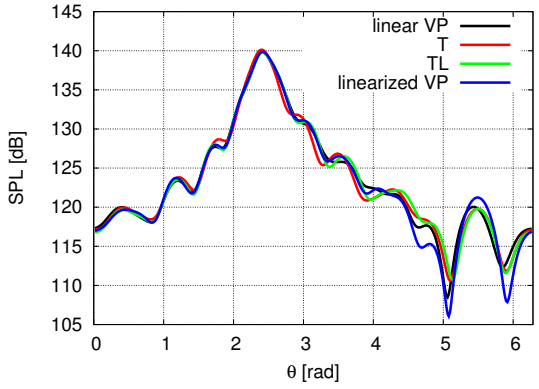

(c) $M = 0.3$

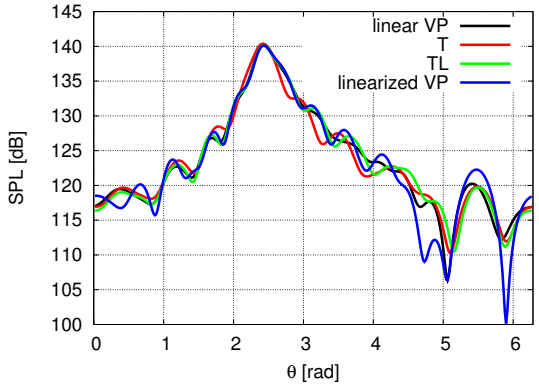

(d) $M = 0.4$

Figure 3: SPL of the acoustic pressure for $\omega/c_0 = 5$.

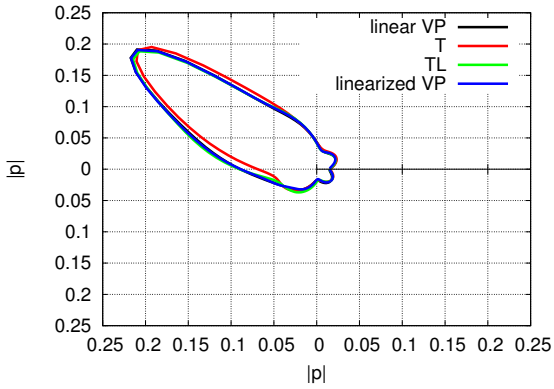

(a) $\omega/c_0 = 2$

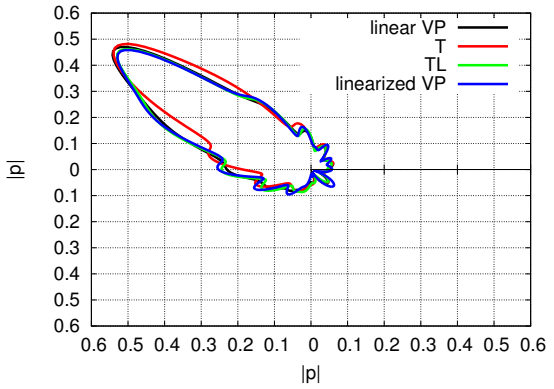

(b) $\omega/c_0 = 5$

Figure 4: Noise directivity pattern for $M = 0.4$.

and for both wave numbers considered. It is worth noting that the T formulation solver used here has been validated against numerical results presented in literature[19] (these results are not shown here for the sake of conciseness).

Finally, a numerical analysis aimed at investigating about the numerical differences between the Taylor-Lorentz formulation and the linearized VP-A4 formulation is performed. These formulations are based upon two different strategies to solve the same differential equation (Eq. 8), which lead to solutions of different level of accuracy. As stated before, the main differences reside in two main aspects: (*i*) the VP-A4 formulation is a boundary-field integral formulation, while the TL formulation is a boundary integral one, and (*ii*) the Green function used in Eq. 14 is the exact fundamental solution of the wave equation in uniform translating flow (Eq. 1), whereas the Taylor-Lorentz Green function (Eq. 10) is an approximated fundamental solution of the wave equation in non-uniform translating flow. Specifically, Figs. 5 and 6 compare the SPL curves computed by the TL formulation, the VP-A4 approach proposed in Section 2.4 and the VP formulation, for the same Mach numbers and wave num-

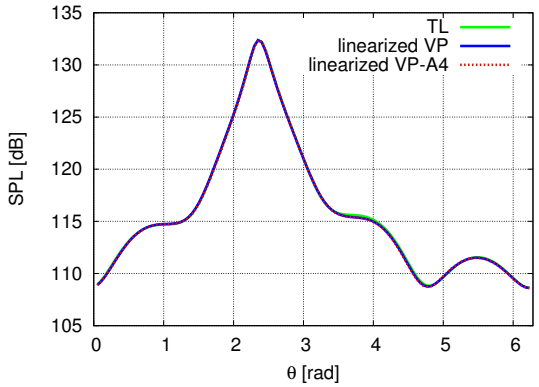

(a) $M = 0.1$

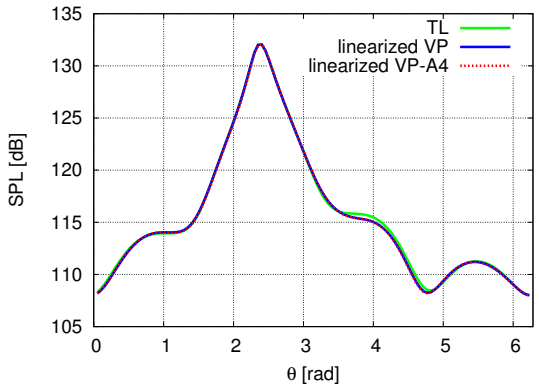

(b) $M = 0.2$

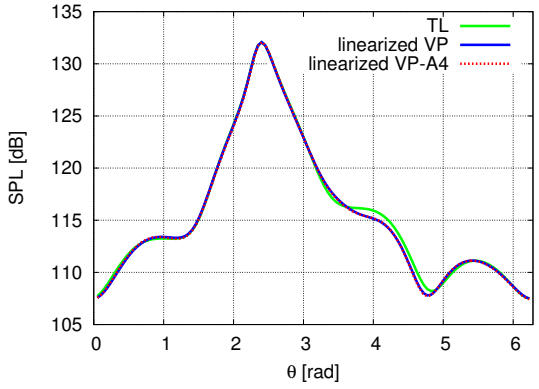

(c) $M = 0.3$

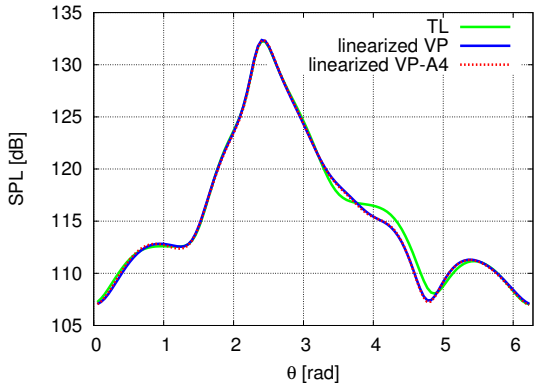

(d) $M = 0.4$

Figure 5: SPL of the acoustic pressure for $\omega/c_0 = 2$.

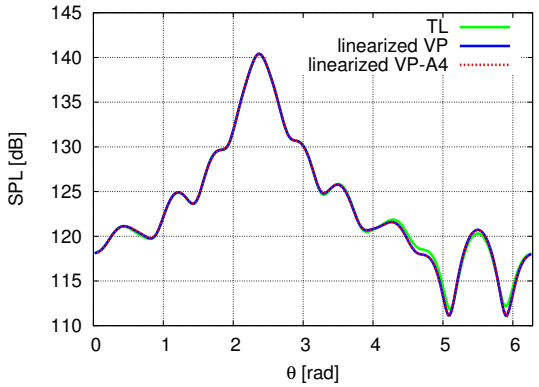

(a) $M = 0.1$

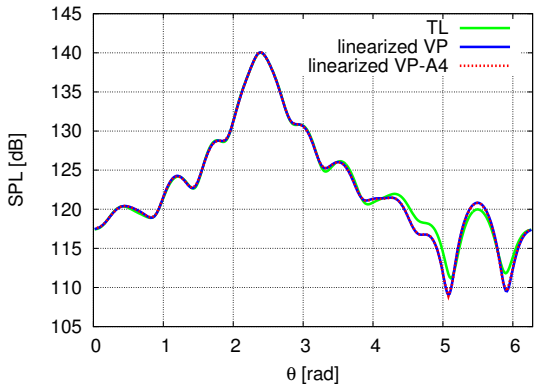

(b) $M = 0.2$

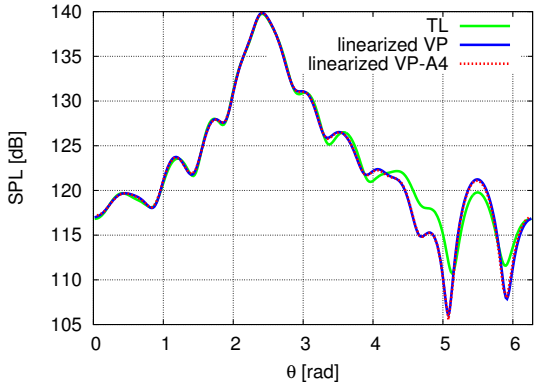

(c) $M = 0.3$

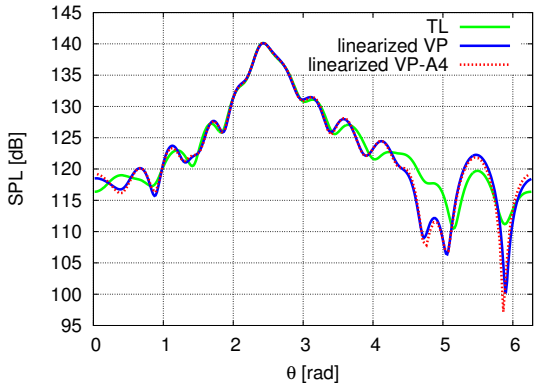

(d) $M = 0.4$

Figure 6: SPL of acoustic pressure the for $\omega/c_0 = 5$.

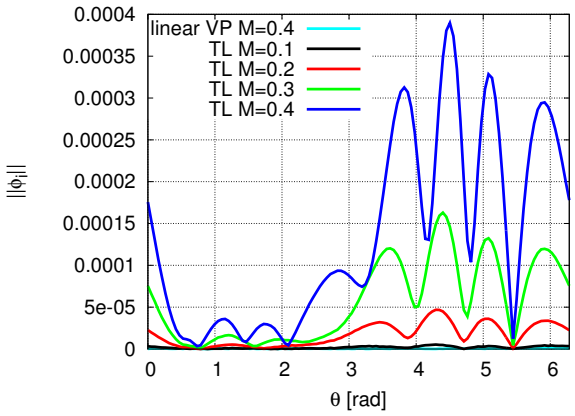

Figure 7: Incident Pressure field radiated by the sphere surface using linear VP and Taylor-Lorentz (T-L) formulations for $\omega/c_0 = 5$ and $d/a = 3$.

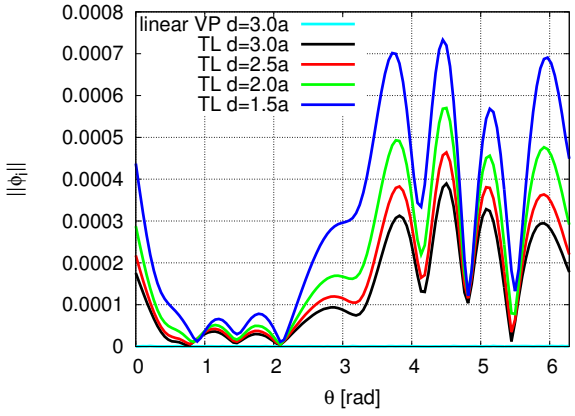

Figure 8: Incident Pressure field radiated by the sphere surface using linear VP and Taylor-Lorentz (T-L) formulations for $\omega/c_0 = 5$ and $M = 0.4$.

bers considered above. These figures demonstrate that VP-A4 predictions are in very good agreement with those provided by the linearized VP approach, whereas some differences appear in the TL formulation, which increase with the increase of both Mach number and wave number. This behavior of the TL-based outcomes can be explained with the use of a fundamental solution of the wave equation for non-uniform translating flow (see Eq. 10) that is not exact, but rather, is affected by approximations depending on Mach number and signal wave number.

The drawback of using an approximated fundamental solution is confirmed by Figs. 7 and 8 which show, for different Mach numbers and observer positions, the incident pressure field radiated by the body surface (that is theoretically equal to zero) predicted by the TL and linear VP models, respectively. For the linear VP formulation the incident pressure field exactly satisfies the integral equation and thus the radiated contribution is numerically zero for all Mach numbers and microphones distances considered. The same is not true for the TL model, for which the incident field contribution from the body surface is not zero and increases with Mach number and frequency values; this contribution becomes more relevant for acoustic observers closer to the scatterer where the assumption of the TL-based formulation, namely $\mathbf{M}_{st} \ll \mathbf{M}_{\infty}$, is scarcely satisfied (in proximity of the body surface the nonuniform flow velocity becomes of the same order of magnitude of the mean uniform flow velocity[16]).

3.2. Noise scattered by helicopter fuselage

This section presents the results of the numerical investigation concerning the effects of sound scattering produced by a Bo-105 scaled model fuselage impinged by the noise radiated by the scaled helicopter main rotor. The configuration examined is that considered within the framework of Hart II program. The main-rotor, having radius $R = 2$ m, operates in a 5.4-deg, low-speed descent flight, with advanced ratio $\mu = 0.15$ and rotational speed $\Omega = 109.12$ rad/sec. Approximately, the fuselage is about 0.5 m wide, 1.0 m high and 3.2 m long. The

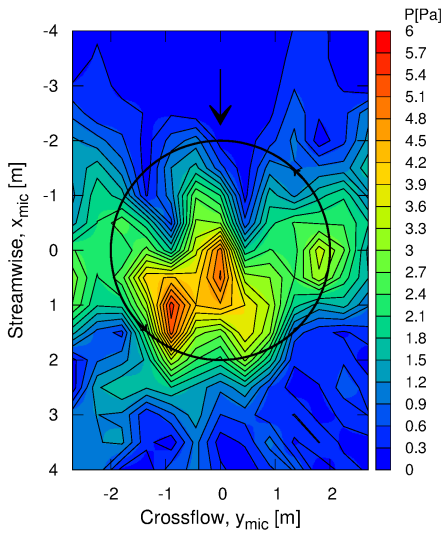

Figure 9: Incident Pressure field radiated by the main rotor at the fifth blade-passage frequency.

results are presented in terms of pressure fields (incident and total) and shielding factor, γ_T, defined as the ratio between the total pressure and the incident one, on a horizontal plane, 5.4 m wide and 8

m long, centered with the rotor hub and placed 2.2 m below the rotor disk.

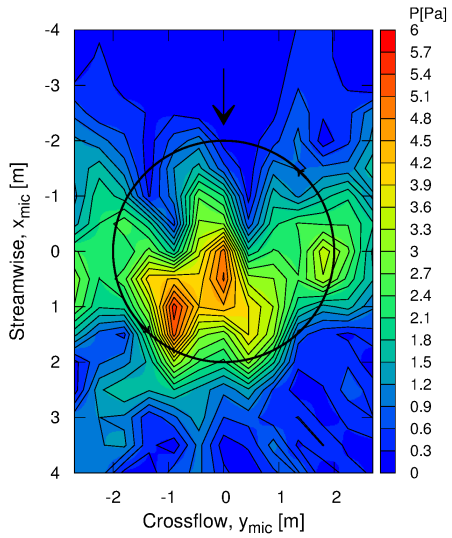

Figure 10: Total Pressure field radiated by the main rotor and the fuselage at the fifth blade-passage frequency.

The main rotor is assumed as a frozen source of noise: indeed, for the working conditions considered, the fuselage is not massively impinged by the rotor wake and hence, although affecting rotor aerodynamics, this occurs to a lower extent. Therefore, first, the acoustic pressure field generated by the main rotor is evaluated as if it were isolated through a tool based on a Boundary Element Method for potential flows that has been extensively validated in the recent past against the HART II database[24,25]; then, the shielding effect of the fuselage on the aeroacoustic perturbation generated by the main rotor is investigated by some of the presented scattering formulations.

Figures 9 and 10 show the contour plot of the incident and total pressure field, respectively, at the fifth blade-passage frequency (BPF) of the main rotor ($k = 6.385$), corresponding to the lower frequency having a wavelength comparable to the fuselage characteristic size. The scattered field is predicted by the linear VP formulation since the effect of the nonuniform flow on the scattering prediction has been proven to be negligible. The comparison between incident and overall pressure maps well highlights that the presence of the fuselage does not affect remarkably the radiated noise; the shielding factor contour plot, not shown here for the sake of conciseness, reveals that it is almost one everywhere on the carpet of microphones. This result agrees with the conclusion of previous works[24,25] stating that the major effect of the fuselage is to modify rotor aerodynamics, and in turns, the incident pressure field radiated by it, rather than to provide a significant direct acoustic contribution.

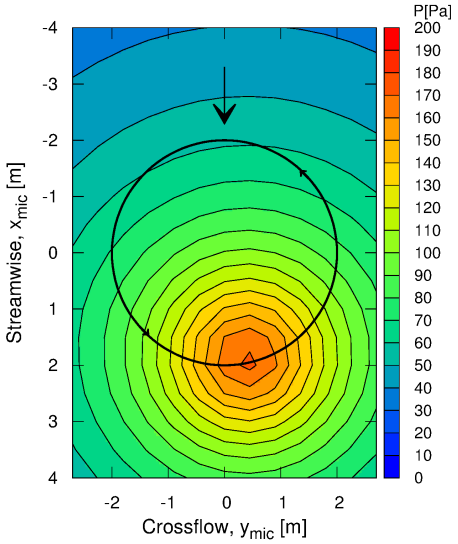

Figure 11: Incident Pressure field radiated by the tail rotor at the second blade-passage frequency.

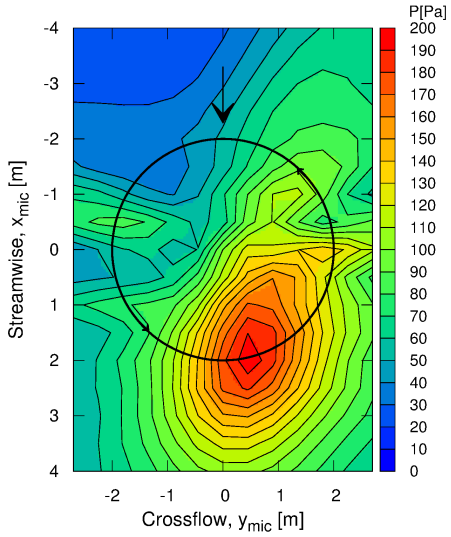

Figure 12: Total Pressure field radiated by the tail rotor and the fuselage at the second blade-passage frequency.

The scattering effect of the fuselage is expected to be considerable at frequencies higher than the fifth BPF for which, however, the corresponding carried energy content is negligible.

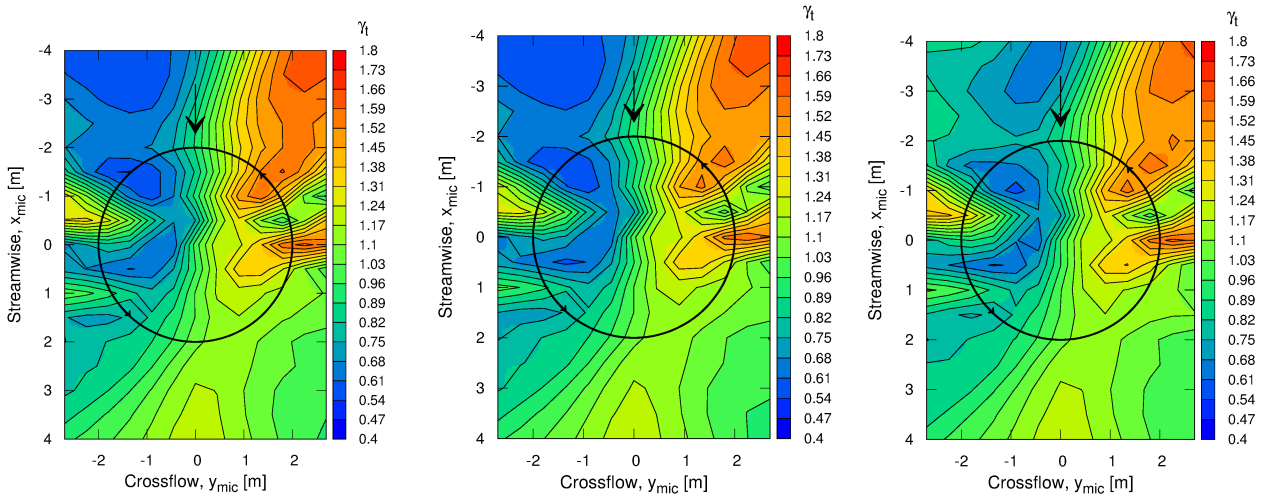

(a) *VP formulation* (b) *TL formulation* (c) *T formulation*

Figure 13: Shielding factor at the second blade-passage frequency.

For a given frequency of the incident field, a different fuselage scattering effect is obtained in function of the disturbance source position: this is due to the different shielding effect occurring in distinct directions of radiation (related to the length of intersection segments between body and direction of noise propagation). For this reason the scattering of the noise emitted by the a tail rotor located at the end of the fuselage is examined. For the sake of simplicity it is represented as a pulsating co-moving harmonic source located at $\mathbf{x}_s = [2\ m, 0.4\ m, -0.9\ m]$ with respect to the hub position. The scattering analysis is performed at the second blade-passage frequency ($k = 6.704$) of the 2-blade tail rotor model scale (the tail-rotor rotational speed is about six times that of the main-rotor). Figures 11 and 12 show the contour plot of the corresponding incident and total pressure field, respectively. As expected, the scattering contribution of the fuselage is not negligible and the total pressure field differs relevantly from the incident one. This in confirmed by figure 13 depicting the shielding factor provided by linear VP, Taylor-Lorentz and Taylor formulations, respectively. The scattered pressure is of the same order of magnitude of the incident one and the effect of the nonuniform mean flow on the solution is practically negligible, as inferred by comparing Figs. 13(a) and 13(b). The agreement among predictions is good, with the main differences located in the region upstream the fuselage. Note that outcomes from the linear VP and TL formulations match very well highlighting some discrepancies with respect to the results predicted by the Taylor formulation.

4. CONCLUSIONS

A theoretical-numerical comparison among different integral formulations aimed at the analysis of propagation of scattered waves in non-uniform potential flows around moving bodies has been proposed. Specifically, the capabilities of three standard formulations (linear VP, Taylor and Taylor-Lorentz) to predict the effects of nonuniform mean flow (due to the scatterer motion) on the acoustic pressure field are investigated and compared with those of two non-standard formulations (linearized VP and linearized VP-A4). One of the main novelties of this paper consists of the introduction of the linearized VP-A4 formulation, which is an alternative boundary-field integral solution of the Taylor-Lorentz convective wave equation in non uniform flows. The main difference between the TL and VP-A4 formulations is related to the fundamental solution used: the exact fundamental solution of the wave equation in uniform translating flows for VP-A4, and the approximated fundamental solution of the wave equation in nonuniform translating flows for TL.

The main outcomes of the analysis are summarized in the following:

- linear VP, Taylor and Taylor-Lorentz formulations give accurate results only for very low Mach numbers and frequencies of the impinging perturbation: indeed, the differences with respect to the predictions of non-standard approaches (linearized VP and linearized VP-A4) increase with the scatterer velocity and wavenumber;

- the Taylor formulation gives accurate results only for $M_\infty \leq 0.2$, showing that the inclusion of M_∞^2-order terms seems to be mandatory also for low Mach number in order to maintain a suitable accuracy of the numerical predictions;
- the use of the exact fundamental solution of the wave equation operator in uniform translating flows in the VP-A4 formulation seems to increase the accuracy of the numerical predictions, which are in good agreement with those of the (more accurate) linearized VP approach. This means that some inaccuracies arise in the Taylor-Lorentz formulation due to the approximated Green function used in the integral formulation;
- the sound scattering investigation concerning a model helicopter cabin demonstrates that the tail-rotor noise field is more remarkably affected by the fuselage presence than that from the main rotor. This is essentially due to the relative position between fuselage and tail rotor which enhances the fuselage scattering effects, in that different shielding effect occurs in different directions of radiation. Otherwise, the aerodynamics of the main rotor is directly affected by the fuselage, whereas the fuselage shielding effect on its radiated noise is negligible. It is also demonstrated that for the low Mach number flight conditions examined the nonuniform flow effects play a marginal role in the acoustic scattering predictions.

ACKNOWLEDGMENTS

The work presented in this paper is part of the activities of Roma Tre University/CNR-INSEAN team within the project GARTEUR HC AG-24.

REFERENCES

[1] C.A. Reimann., A.F. Tinetti, M.H. Dunn, Noise Scattering by the Blended Wing Body Airplane: Measurements and Prediction, *AIAA Paper 2006-2474, 12th AIAA/CEAS Aeroacoustics Conference*, Cambridge, Massachusetts, 2006.

[2] S. Lee, K.S. Brentner, P.J. Morris, Time-Domain Approach for Acoustic Scattering of Rotorcraft Noise, *Journal of the American Helicopter Society*, 57(4) (2012) 1-12.

[3] 28th ITTC, "Final Report and Recommendations of the Specialist Committee on Hydrodynamic Noise", *Proc. of the 28th Tank Conference*, Volume II, WUXI, China, September 17-22, 2017.

[4] Wang, T.Q., and Zhou, S., "Investigation on Sound Field Model of Propeller Aircraft Effect of Vibrating Fuselage Boundary," *Journal of Sound and Vibration*, Vol. 209, No. 2, 1998, pp. 299-316.

[5] Schenck, H.A., "Improved Integral Formulation for Acoustic Radiation Problems," *Journal of the Acoustical Society of America*, Vol. 44, No. 1, 1968, pp. 41-58.

[6] Seybert, A.F., and Soenarko, B., "Radiation and Scattering of Acoustic Waves from Bodies of Arbitrary Shape in Three-Dimensional Half Space," *Journal of Vibration, Acoustics, Stress, and Reliability in Design*, Vol. 110, No. 1, 1988, pp. 112-117.

[7] Y.Z. Kehr, J.H. Kao, Underwater Acoustic Field and Pressure Fluctuation on Ship Hull Due to Unsteady Propeller Sheet Cavitation, *Journal of Marine Science and Technology*, 16(3) (2011) 241–253.

[8] T.Q. Wang, S. Zhou, Investigation on Sound Field Model of Propeller Aircraft âĂŞ The Effect of Vibrating Fuselage Boundary, *Journal of Sound and Vibration*, JSV 209 (2) (1998) 299-316.

[9] S. Lee, K.S. Brentner, P.J. Morris, Acoustic Scattering in the Time Domain Using an Equivalent Source Method, *AIAA Journal*, 48(12) (2010) 2772–2780. doi: 10.2514/1.45132

[10] M. Gennaretti, C. Testa, A Boundary Integral Formulation for Sound Scattered by Moving Bodies, *Journal of Sound and Vibration*, 314(3, 5) (2008) 712-737.

[11] Y. Mao, Y. Gu, C. Xu, Validation of Frequency-Domain Method to Compute Noise Radiated from Rotating Source and Scattered by Surface, *AIAA Journal*, 54(4) (2016) 1188–1197. doi:10.2514/1.J053674

[12] Gennaretti, M., Bernardini, G., Poggi, C., and Testa, C. "A Boundary-Field Integral Formulation for Sound Scattering of Moving Bodies," *Proceedings of the 22nd AIAA/CEAS Aeroacoustics Conference*, AIAA Paper 2016-2715, Lyon, France, 2016.

[13] Gennaretti, M., Bernardini, G., Poggi, C., and Testa, C. "Lighthill Equation-based Boundary Integral Formulations for Sound Scattering of Moving Bodies," *23nd AIAA/CEAS Aeroacoustics Conference*, AIAA Paper 2017, Denver, CO, 2017.

[14] Taylor, K. "A transformation of the acoustic equation with implications for wind-tunnel and low-speed flight tests." *Proceedings of the Royal Society of London A: Mathematical, Physical and Engineering Sciences*, Vol. 363. No. 1713. The Royal Society, 1978.

[15] Astley, R. J., and J. G. Bain. "A three-dimensional boundary element scheme for acoustic radiation in low mach number flows." *Journal of Sound and Vibration* 109.3 (1986): 445-465.

[16] Mancini, Simone, et al. "An integral formulation for wave propagation on weakly non-uniform potential flows." *Journal of Sound and Vibration* 385 (2016): 184-201.

[17] Morino, L., and Gennaretti, M., "Boundary Integral Equation Methods for Aerodynamics," in: S.N. Atluri (Ed.), Computational Nonlinear Mechanics in Aerospace Engineering, *Progress in Astronautics and Aeronautics*, Vol. 146, AIAA, 1992.

[18] Morino, L., and Gennaretti, M., "Toward an Integration of Aerodynamics and Aeroacoustics of Rotors," *Proceedings of the DGLR/AIAA 14th Aeroacoustics Conference*, AIAA Paper 92-02003, Aachen, Germany, 1992.

[19] Mayoral, Salvador; Papamoschou, Dimitri. "Prediction of jet noise shielding with forward flight effects". *51st AIAA Aerospace Sciences Meeting including the New Horizons Forum and Aerospace Exposition* 2013. p. 10.

[20] van der Wall, Berend G. "2nd HHC aeroacoustic rotor test (HART II)-Part I: Test Documentation." Tech. Rep. IB 111-2003/31, DLR (2003)

[21] van der Wall, B. G., Burley, C. L., Yu, Y., Richard, H., Pengel, K., and Beaumier, P., "The HART II Test-Measurement of Helicopter Rotor Wakes," *Aerospace Science and Technology*, Vol. 8, No. 4, 2004, pp. 273-284.

[22] van der Wall, B. G., and Burley, C. L., "2nd HHC Aeroacoustic Rotor Test (HART II)-Part II: Representative Results," Tech. Rep. IB 111-2005, DLR, 2005.

[23] Gennaretti, M., Bernardini, G., "Novel Boundary Integral Formulation for Blade-Vortex Interaction Aerodynamics of Helicopter Rotors," *AIAA Journal*, Vol. 45, No. 6, 2007, pp. 1169-1176.

[24] Gennaretti, M., Bernardini, G., Serafini, J., Romani, G. Assessment of a comprehensive aeroacousto-elastic solver for rotors in BVI conditions. *In 43nd European rotorcraft forum.*

[25] Gennaretti, M., Bernardini, G., Serafini, J., Romani, G., 'Rotorcraft Comprehensive Code Assessment for Blade–Vortex Interaction Conditions,' *Aerospace Science and Technology*, Vol. 80, 2018, pp. 232–246. doi: 10.1016/j.ast.2018.07.013.